

A CENTRIFUGE INVESTIGATION OF TWO DIFFERENT SOIL- STRUCTURE SYSTEMS WITH ROCKING AND SLIDING ON DENSE SAND

Iason Pelekis¹, Gopal S. P. Madabhushi², and Matthew J. DeJong¹

¹ University of Cambridge, Department of Engineering
Trumpington Street, Cambridge, CB2 1PZ
e-mail: {ip312, mjd97}@cam.ac.uk

² University of Cambridge, Department of Engineering
Schofield Centre, High Cross, Madingley Road, Cambridge, CB3 0EL
mspg1@cam.ac.uk

Keywords: Earthquake, Centrifuge Testing, Soil-Structure Interaction, Structural Rocking, Foundation Rocking.

Abstract. *Seismic protection of structures by means of rocking isolation is becoming increasingly popular, because allowing uplift is an inexpensive way to reduce structural demand. However, understanding the role of soil–structure interaction in the response of rocking systems is important to define what type of rocking system might be most effective. To address this challenge, a campaign based on centrifuge modelling and testing is currently ongoing. The primary objective is to assess the force demand that rocking systems experience during their motion. Flexible structures that rock while stepping on discrete footings (structural rocking) and flexible structures with discrete footings rocking on soil (foundation rocking) are both considered. Following this distinction, two building models were designed with the only difference being the connectivity of the columns to the footings. For structural rocking, columns were designed to detach and step on their footings, while for foundation rocking the footing-column connection was designed to be rigid. The two building models were tested side-by-side in a centrifuge. A second test was also conducted, where thin steel “fuses” were installed in the interface of structural rocking, to further study the allocation of energy dissipation between structural elements and fuses, and soil medium. The building models were placed on the surface of dense sand and then tested using sinusoidal ground motions which caused a combination of sliding and rocking. The global response of the models in terms of overturning moment and storey shear was investigated and back validated by obtaining directly the internal loads, which were found capped regardless of the extent of rotation. Moreover, the base isolation effect was evident during large amplitude resonant excitations, whereas during a low frequency low amplitude excitation there was no clear benefit of rocking. Finally, no significant effect was observed in limiting the base shear demand by using the steel fuses.*

1 INTRODUCTION

In areas prone to earthquakes of catastrophic magnitude, the current design approach of damage tolerance may result in poor structural performance regarding repair costs, downtime and business disruption. For example, the Christchurch earthquake in New Zealand has led building stakeholders to ask for improved seismic performance and damage mitigation technologies, to avoid disruption, economic losses and dependence on insurance in future earthquakes [1]. Similarly, in the aftermath of Chile's 2010 earthquake, it was concluded that "*efforts still need be made for better construction practices*", while the economic losses reached a third of the country's gross domestic product [2]. Consequently, design objectives are now becoming more stringent, incorporating economic and social implications of earthquake damage.

Seismic protection by means of rocking isolation is becoming increasingly popular, since allowing uplift is an inexpensive way to reduce structural damage demand. Structures idealized as rigid rocking blocks were studied by Housner [3] back in the 1960s. Since then, the overturning tendency and self-centering nature of rocking [4, 5], the implementation of rocking with dampers to suppress swaying motion [6–15], the coupling of flexibility and rocking, [16–19] and the role of the higher modes [17, 18, 20, 21] have been studied both from an experimental and analytical point of view, with a clear focus on the structural performance (structural rocking). In practice, while the base shear reduces due to structural rocking, excitation due to impacts at the interface of the stepping mechanism might amplify internal loads significantly. Parallel to these studies, there has been extensive research on the response of rocking foundations which utilize soil as an energy dissipater and are combined with an admissible failure mechanism of their superstructure (foundation rocking). The uplifting and earthquake response [22–26], the achieved damping [15, 27] and the parameters of soil and superstructure regarding structures with rocking foundations [28] lead to the conclusion that the more a foundation is allowed to rock, the lesser can be the damage in the superstructure, but this will come at the expense of larger displacements and residual differential settlements.

The objective of this paper is to examine the force demand of two small scale flexible building models that can rock above (model RA, structural rocking) or below their foundation level (model RB, foundation rocking), including soil-structure interaction effects, based on observations from centrifuge testing (Figure 1). The design of the two rocking models are first presented, including the design of an energy dissipation element (fuse) used in structural rocking. The models were first tested side-by-side and on a separate test two yielding plates were installed to act as energy dissipating fuses in the RA model. Having subjected the models to multi-frequency ground excitations, the internal loadings from structural components were examined and the potential base isolation effect against typical fixed base oscillators were quantified.

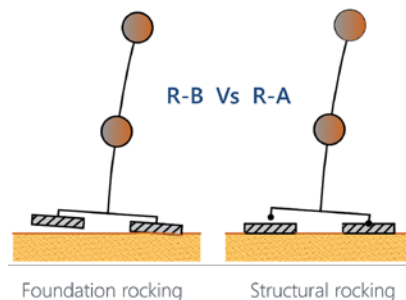


Figure 1: Two models of flexible structures (2DOF) rocking on discretized footings and soil, below the foundation level (left) and above that (right).

2 DESIGN OF ROCKING MODELS

Two linear elastic building models were designed as identical, with their only difference being the connectivity of their columns to the footings (Figure 2). For the model rocking above the foundation (RA), columns were designed to detach and step on their footings, while for the model rocking below the foundation (RB) the footing-column connection was designed to be rigid. While not in rocking action and assuming the soil-footing interface as a fixed boundary, the RA and RB models correspond to a hinged base frame and a fixed base frame, respectively.

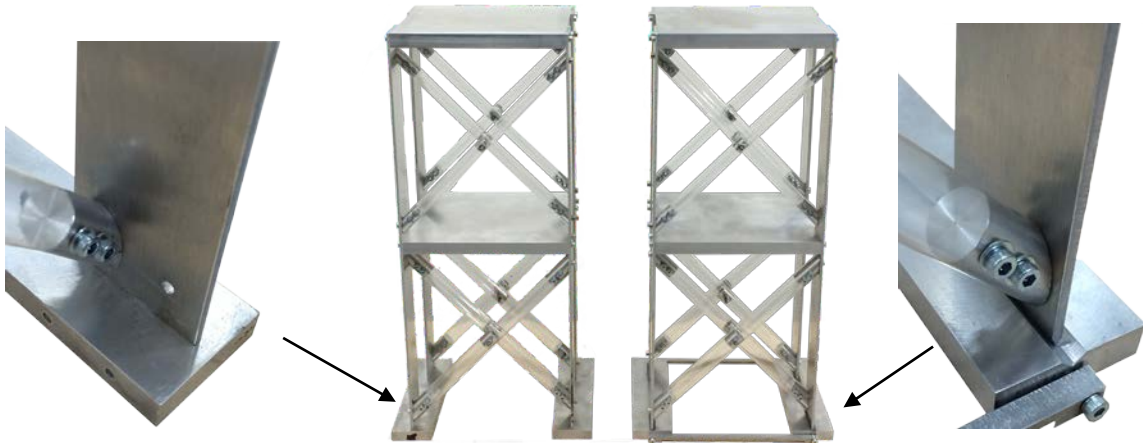


Figure 2: Column fixed to column for foundation rocking (far left), rocking below the foundation model (RB, left), rocking above the foundation (RA, right), connection for hinged support and structural rocking (far right).

The overall dimensions, the sizing of the members and the dynamic response properties are governed by a combination of factors covering the experimental needs and relating the models to a prototype building (Table 1, Figure 3). Therefore, in prototype scale, the models represent 3-4 storey buildings with a natural period of 0.70s (1.4Hz). Such buildings are represented well by their first two lateral modes in unidirectional ground shaking and therefore, the centrifuge models were designed as 2DOF oscillators for shaking and rocking in one direction. Moreover, the distance between the discrete footings is larger than two times a footing's width to avoid generating a mat foundation response. This also applies to the side-by-side testing for adjacent footings to minimize structure-soil-structure interaction of the models in the centrifuge box (Figure 3).

Properties	Fixed base (RB)	Hinged base (RA)
First mode period (prototype)	0.66s	0.70s
Experimental first mode frequency (model)	53Hz	46Hz
Experimental second mode frequency (model)	147Hz	136Hz
Design stiffness (proto- type)		
Top storey	7.9MN/m	7.9MN/m
Bottom storey	16.5MN/m	15.9MN/m
Design stiffness (mod- el)		
Top storey	0.24MN/m	0.24MN/m
Bottom storey	0.50MN/m	0.48MN/m
Total superstructure mass (prototype)	60 metric tonnes	
Dynamic storey mass (model)	0.83kg	
Slenderness ratio	0.25	
Bearing pressure	80kPa/footing, FoS=2.3 (DA1/2 [29])	
Experimental centrifuge scale	33	

Table 1: Basic properties of the buildings models subjected to centrifuge testing

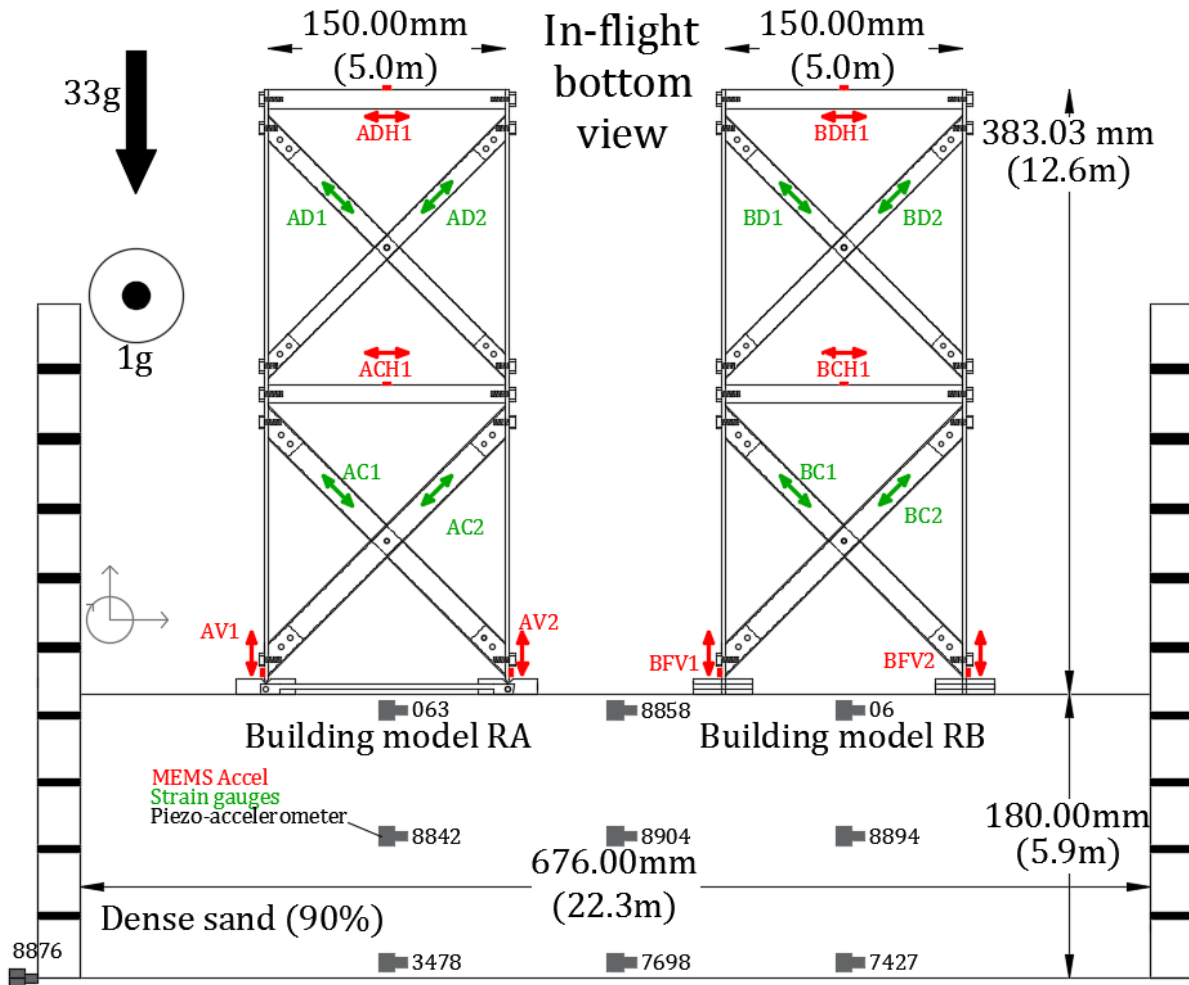


Figure 3: Side-by-side centrifuge testing and overall dimensions of the models RA and RB

To design the members two load cases were considered. Those consisted of the case at which the models are at the onset of uplift and the case at which the maximum rocking angle is achieved before toppling, that is the slenderness angle. For the first load case, a linear elastic response was assumed and a spectral acceleration was identified iteratively, so that a zero-tension load in the uplifting columns was achieved. The design base shear was identified for this spectral acceleration, as this shear is capped by rocking; the maximum base shear should not be larger than the value at the onset of uplift. For the second load case, when rocking develops the weight of the structure is transferred to the soil through the columns of the one side of the structure. These columns were designed for the increased compressional forces due to this redistribution of loading.

All columns (6082-T6) and bracing elements (plastic PETG tube sections) were designed as linear elastic to avoid masking the rocking action with local failures (e. g. material failure) or other out of interest nonlinear events (e. g. buckling). The key in the similarity of the natural frequencies stems from the bracing configurations which form the primary lateral load resistance mechanism prior uplift. By minimizing the columns' width, the lateral stiffness prior uplift is governed by the bracings, regardless of the boundary conditions at the column base (fixed base or hinged base). This allows for a direct comparison between the two models, with only the parameter of the type of rocking mechanism to be the governing factor causing any potential differences in the earthquake response. The linear elastic performance of the PETG bracing elements and their connections in axial cyclic loading were tested and verified experimentally.

An energy dissipation element was also designed to be installed into the RA model, for a separate side-by-side testing with the RB model. This is a steel tapered plate (S275, Figure 4) which deforms in bending. Its root is bolted to the footing while its free end is linked to the column tip. When the column tip uplifts once rocking initiates, the fuse deforms in bending and dissipates energy due to hysteresis. The performance of this element was predicted computationally and was verified experimentally prior its installation into the RA model (Figure 4).

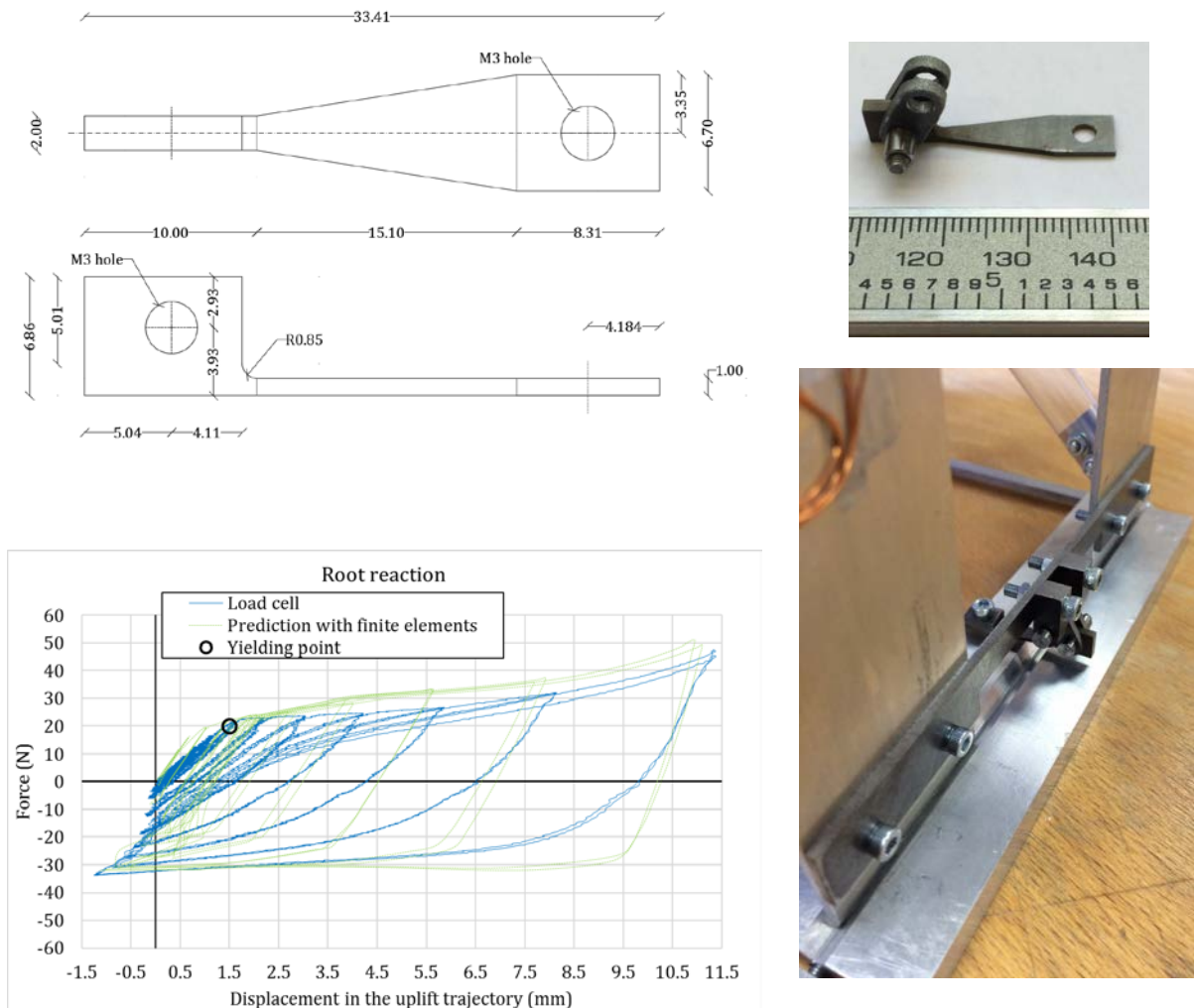


Figure 4: Detailing of the energy dissipation steel plate (top left), steel plate with additional linkage rod (top right), cyclic performance of plate-rod assembly (bottom left), plate installed into model RA (bottom right)

3 EXPERIMENTAL PROGRAM FOR CENTRIFUGE TESTING

The testing of the rocking performance involved two separate centrifuge flights. The setup (Figure 3) of the first flight (Test 1) involved the models RA and RB simply resting (with no embedment) on dense sand ($D_r=90\%$) and allowing them to slide and rock upon the earthquake excitation. The setup of the second flight (Test 2) was the same, with the only difference being that a fuse was installed at each footing of the model RA.

The earthquake response of the models was monitored in terms of accelerations and internal loadings. Micro-Electro-Mechanical System (MEMS) accelerometers were used to monitor the storey lateral accelerations and the vertical acceleration due to impact on the interface of rocking. The PETG bracing elements were essentially converted to load cells, by calibrat-

ing strain gauges that clearly registered the axial strain due to the axial tension or compression of their tube sections. In addition, a series of piezo-electric accelerometers were used to monitor the centrifuge box input excitation and the ground excitation below the foundation level of each model.

The input excitations, measured near the sand surface and between the models, consisted of weak and large amplitude multi-frequency motions (Table 2, Figure 5). In Test 1, a weak ground motion was used first, followed by a strong motion with the target excitation frequency equal to 50Hz to induce resonance. In Test 2, the same input motions were specified, followed by a third motion with a lower frequency content. In both tests, higher harmonics of the centrifuge beam-actuator-package system developed, which were at similar frequencies of the models. The weak motions (EQ-1) were specified to induce a linear elastic response and hence produce a control dataset. The strong motions (EQ-2) and the low frequency motion (EQ-3) were used to induce the uplift of the models.

TEST	EQ	CODE	PGA Model (Pro- TOTYPE)	TARGET FREQUENCY	TESTING
1	1	TEST-1 EQ-1	1.9g (0.06g)	50Hz low amplitude	RA w/o fuse VS RB
1	2	TEST-1 EQ-2	23g. (0.70g)	50Hz large amplitude	RA w/o fuse VS RB
2	1	TEST-2 EQ-1	2.1g (0.06g)	50Hz low amplitude	RA w fuse VS RB
2	2	TEST-2 EQ-2	20.3g (0.61g)	50Hz large amplitude	RA w fuse VS RB
2	3	TEST-2 EQ-3	11.0g (0.33g)	35Hz low amplitude	RA w fuse VS RB

Table 2: Input motion details and model’s testing configuration

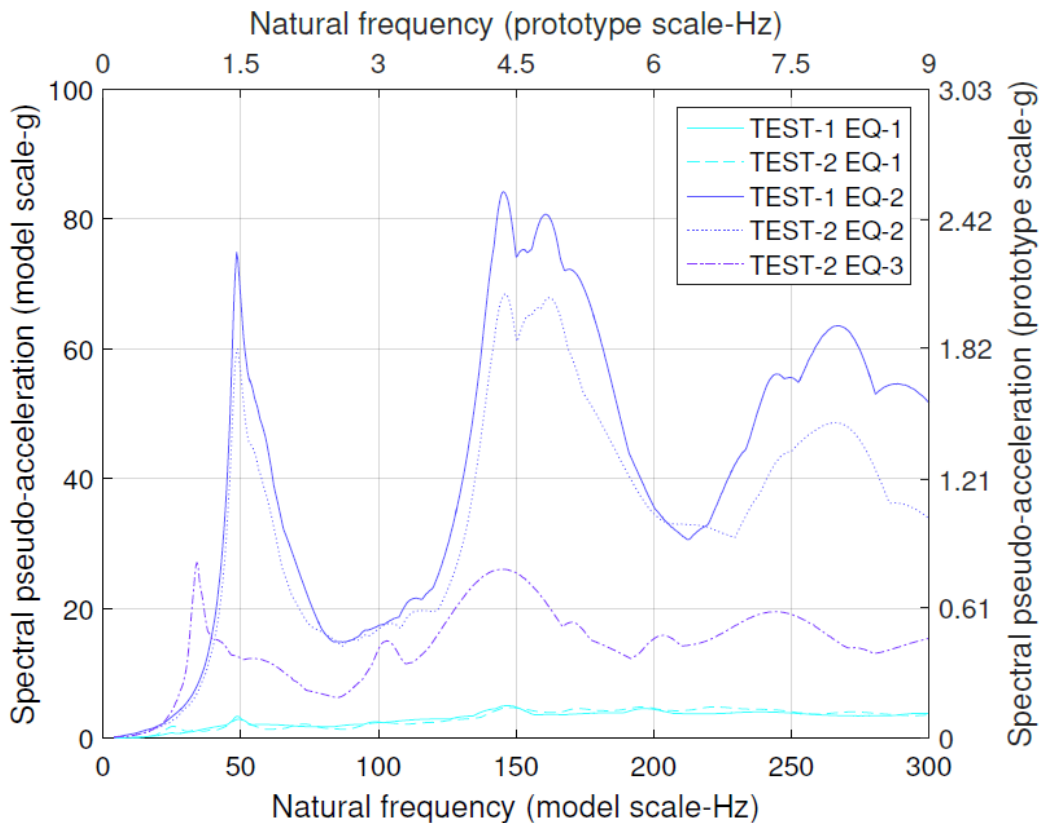


Figure 5: Spectral pseudo acceleration of each ground motion measured on the sand surface, between the models (damping ratio, $\zeta=5\%$)

4 RESULTS

4.1 Verification of uplift and observed response

A sequence of strong impacts was detected by the accelerometers monitoring the vertical movement of the column tips near the footings. Those sequences appeared with a close to zero magnitude in the weak earthquakes, whereas they were very strong during the larger magnitude earthquakes suggesting that uplift and consequently rocking action developed (Figure 6). Analyzing the frequency content of the vertical accelerations and of the lateral acceleration below the soil surface, reveals that the excitation frequencies drove the rocking motion in both models.

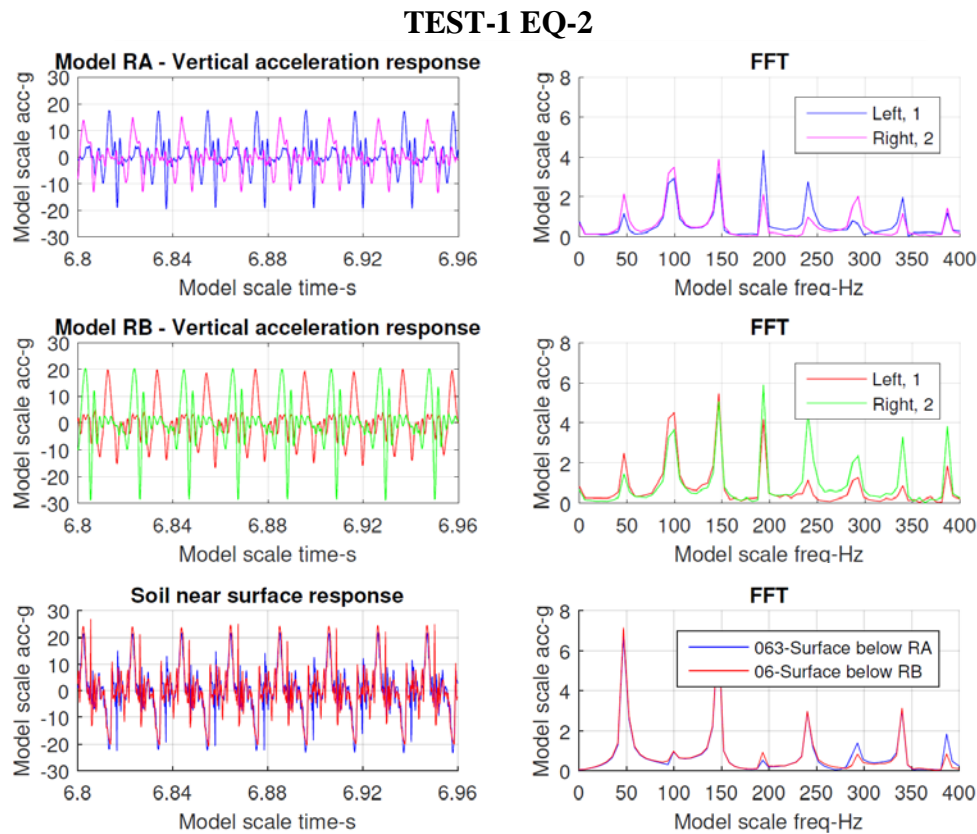


Figure 6: Vertical acceleration response at the column tips as measured from the accelerometers during the steady state in TEST-1 EQ-2 (model scale, 33g)

In other words, as expected, during the small amplitude earthquakes, the response of both models was linear elastic. During the large amplitude earthquakes and the low frequency earthquake, the models rocked and impacts occurred. Model RB was observed to slide during the shaking on the sand surface with a mixed motion of rocking and sliding, with this combination being more evident in the low frequency excitation, and leading to small acceleration demands (Figure 7). On the contrary, the footings of the model RA stayed in position and therefore rocking was developed by that model with partial lateral sliding of the column tips into the grooves of the footings. During the large amplitude earthquakes and low frequency earthquake, the time-history accelerations suggest an out of phase storey profile, which if combined with the existence of the impacts, it further suggests the development of an uplifted mode of vibration [18, 30], driven by the input motion frequencies.

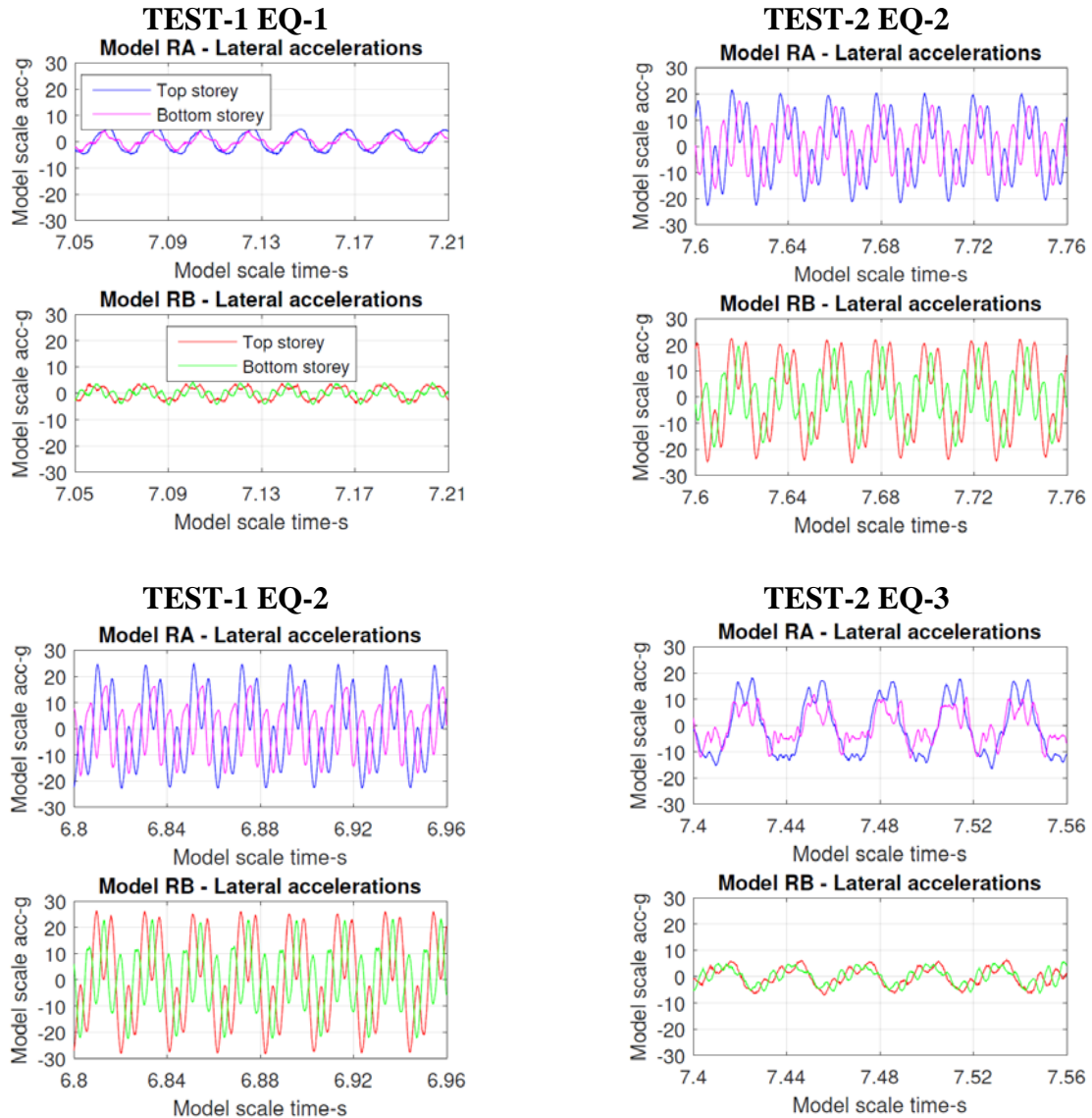


Figure 7: Steady state storey lateral acceleration response (model scale, 33g)

4.2 Moment – rocking angle response

By integrating twice the acceleration trace of the vertical accelerometers at the base of the models, an approximation of the rocking angle was obtained, informative of the extent of rocking that developed. The restraining moment was calculated as the difference of the overturning moment and the rotational acceleration component of the storey slabs which was calculated directly by using the storey horizontal acceleration records.

During the small magnitude earthquakes, both models developed a restraining moment smaller than the required one to cause uplift (Figures 8, 9). During earthquakes EQ-2, the responses of model RA were very similar, indicating that the uplift during rocking was too small to push the fuse to its yielding point (Figure 8). However, after inspection at the end of Test 2, a residual deflection of 0.1mm was measured at the free end of the fuses, which is smaller than the deflection at the yielding point (Figure 4). Considering that during EQ-3 model RA experienced larger rotations than in EQ-2 (Figure 8), it is indicated that EQ-3 was the excitation which activated the fuse noticeably, but still not to the extent a long plastic plateau could develop regarding the local response of the fuses (Figure 4).

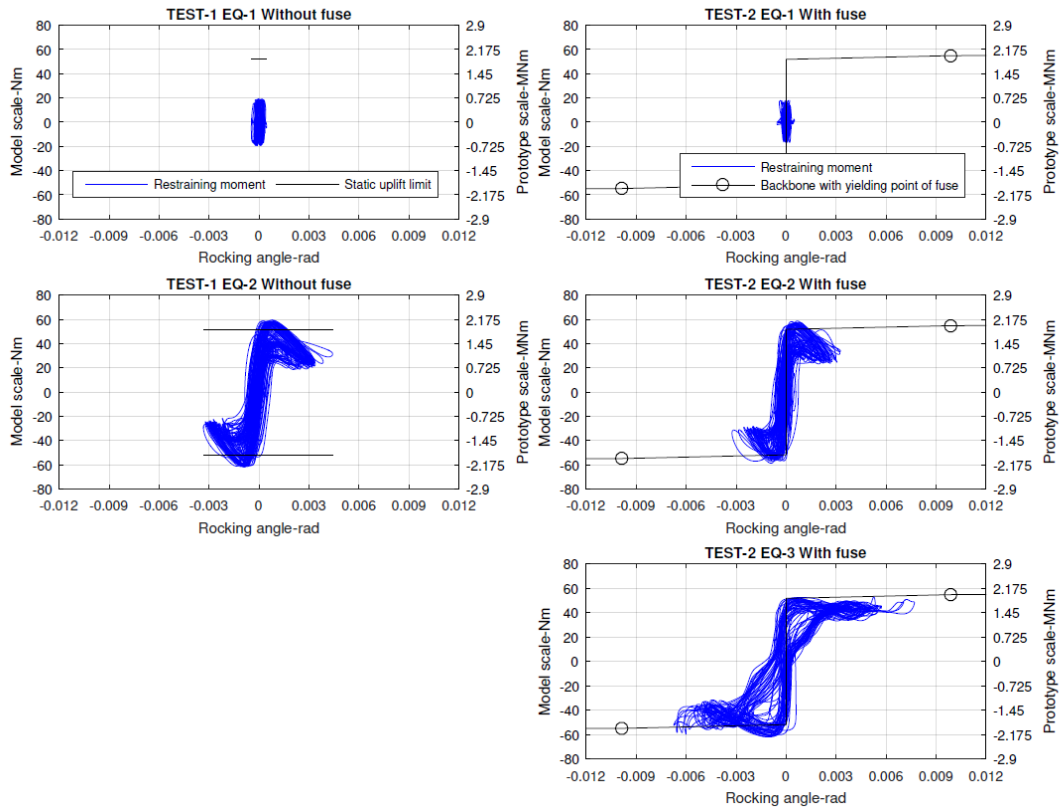


Figure 8: Restraining moment versus rocking angle. Response of model RA during the first test without the fuse (left column) and during the second test with the fuse (right column)

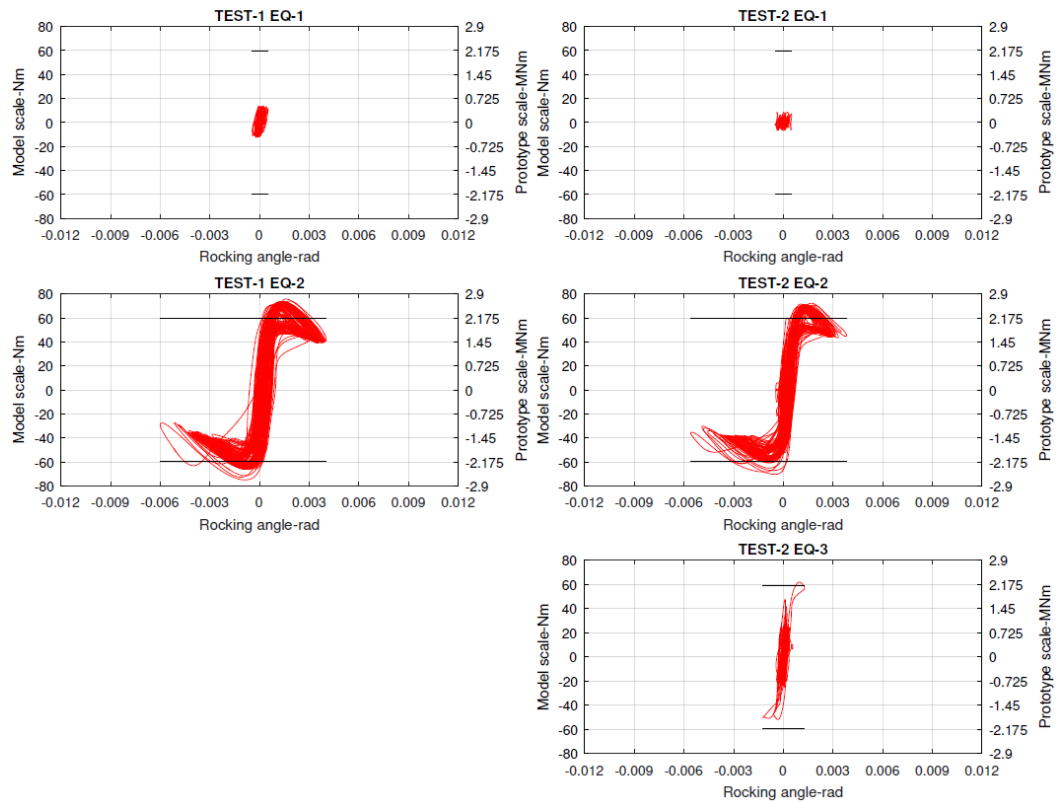


Figure 9: Restraining moment versus rocking angle. Response of the model RB during the first test (left column) and during the second test (right column).

Both models developed transient responses which extended the amount of rotation of the rocking angle initially, whereas the steady state response, represented by the dense loops in Figures 8 and 9 led to smaller rotations. The amount of rotation was similar for both models during the large amplitude earthquakes during both tests. However, during the low frequency earthquake model RB experienced significantly smaller rotations than model RA, although extensive sliding occurred at the same time.

4.3 Storey and bracing response

The load demand on the structure was estimated by utilizing the storey accelerometers and was validated with the strain gauges on the bracing members. From the measurements obtained from the accelerometers (Figures 10, 11), it was observed during the larger magnitude earthquakes, the top storey shear was capped and was found to reduce to zero at the extreme angle of rocking that was experienced by both models. Regarding the RA model during the low frequency excitation, the top storey shear was bound between a maximum and a non-zero minimum value. For the RB model, only the initial transient terms reached the extreme rocking angle during the low frequency earthquake, again due to the subsequent sliding that occurred. The base shear plots were also found to reflect the trend obtained from the restraining moment.

The shear force trends were reflected in the load response of the bracing elements generated by the strain gauges on them. Figures 10 and 11 show that, while the axial force of the top storey bracings was fairly symmetric about the zero-force axis, the bottom storey bracings followed an asymmetric response in the force axis of the plots. In particular, at the extreme angle the models were supported on only one side, with the axial members coinciding at the point of rotation experiencing increased compressional forces. The superstructure weight redistributes due to contact loss on the uplifting side, where the tensional force of the bracing element there dropped to zero. Moreover, the force values that bound the performance of the bracings were constant and the same for both models, indicating that the extent of the rocking angle is of little importance when assessing the load demand once the uplift and rocking begins.

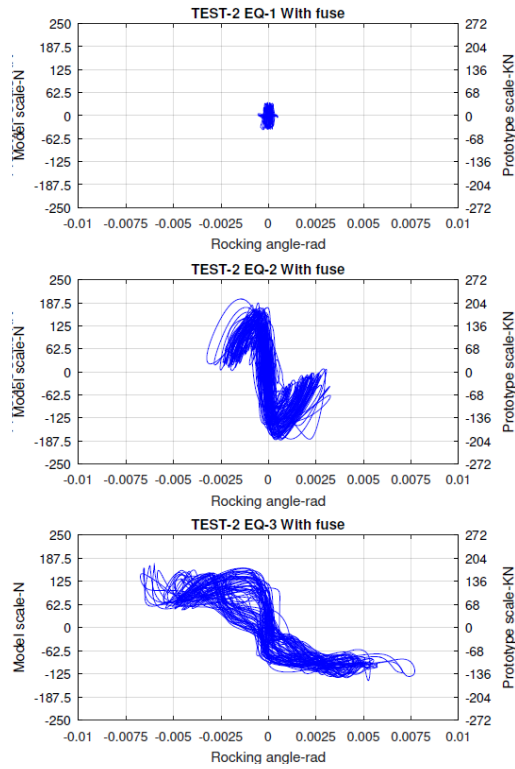
4.4 Base isolation effect

The quantification of the base isolation effect was carried out in terms of base shear values. By using the recorded acceleration on the sand surface, the SDOF response spectra were created. Then, by using the SRSS method with the range of damping ratios obtained from the free vibration traces of the storey accelerations and bracings, the base shear maxima were estimated for similar (hypothetical) fixed base 2DOF models. The estimations were then compared with the base shear maxima directly obtained from the response accelerations (Figure 12). It was found that the base isolation effect was clear during the large amplitude earthquakes, while it was minimal during the low frequency earthquake for both models (Table 3). Finally, the installation of the fuses in model RA did not contribute in any apparent reduction in the base shear demand as observed from the results of Table 3 between the first and second tests for the earthquakes EQ-2.

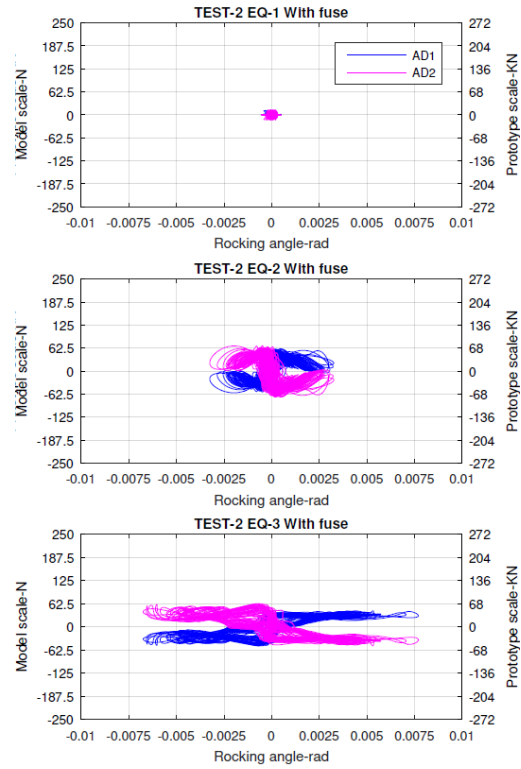
5 CONCLUSIONS

The dynamic soil-structure interaction of twin small scale buildings with foundation rocking and structural rocking was investigated in a proof of concept pilot centrifuge experiment. The following conclusions were drawn:

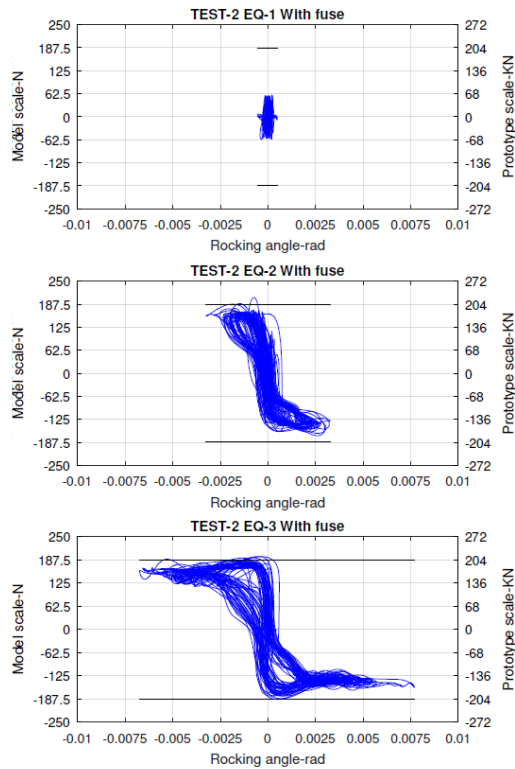
MODEL RA TOP STOREY SHEAR



MODEL RA TOP BRACINGS



MODEL RA BASE SHEAR



MODEL RA BASE BRACINGS

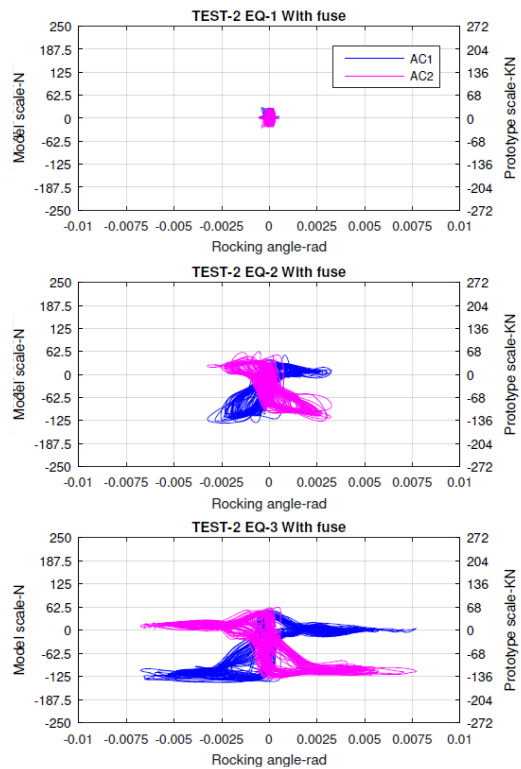
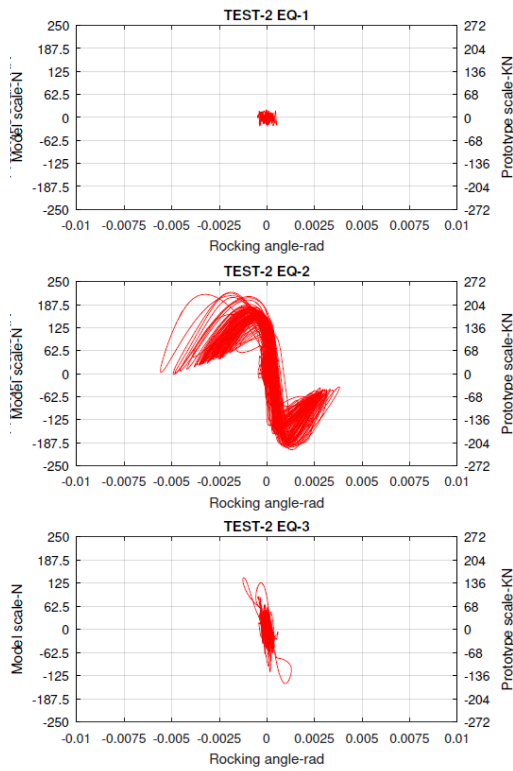
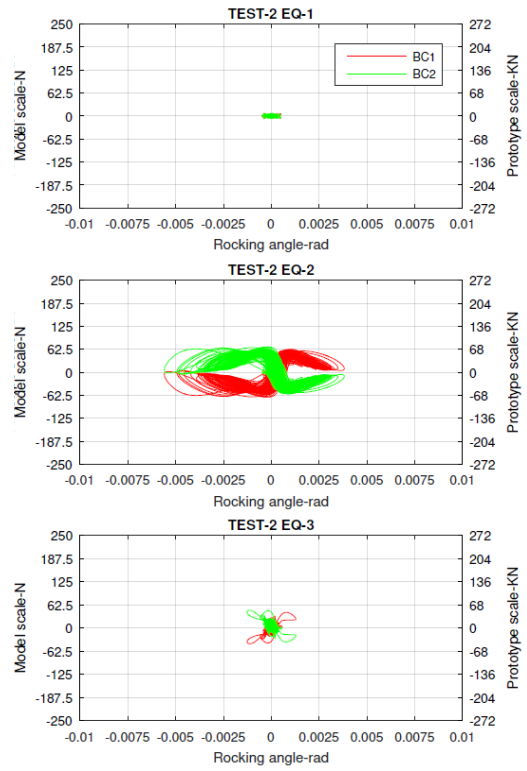


Figure 10: Model RA, top storey shear response (left top) and corresponding bracing axial response (right top), bottom storey shear response (left bottom) and corresponding bracing axial response (right bottom)

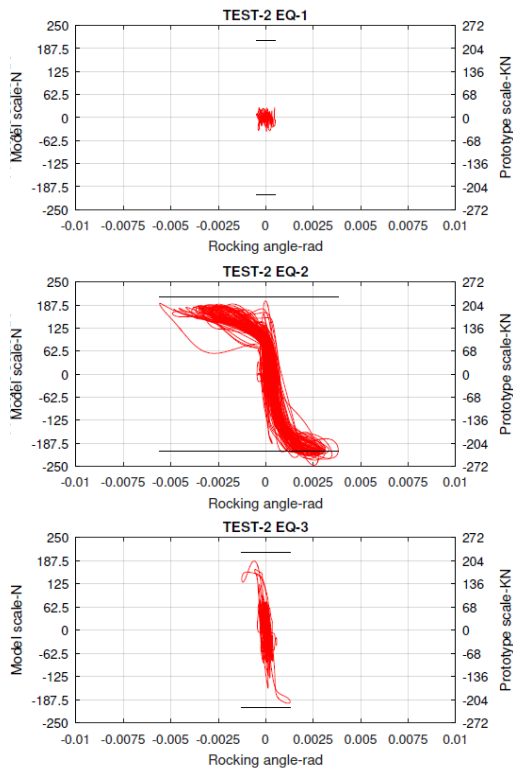
MODEL RB TOP STOREY SHEAR



MODEL RB TOP BRACINGS



MODEL RB BASE SHEAR



MODEL RB BOTTOM BRACINGS

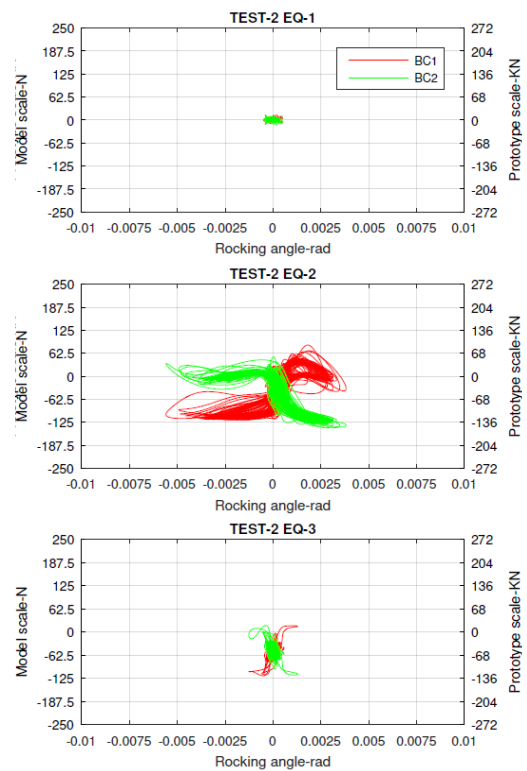


Figure 11: Model RB, top storey shear response (left top) and corresponding bracing axial response (right top), bottom storey shear response (left bottom) and corresponding bracing axial response (right bottom)

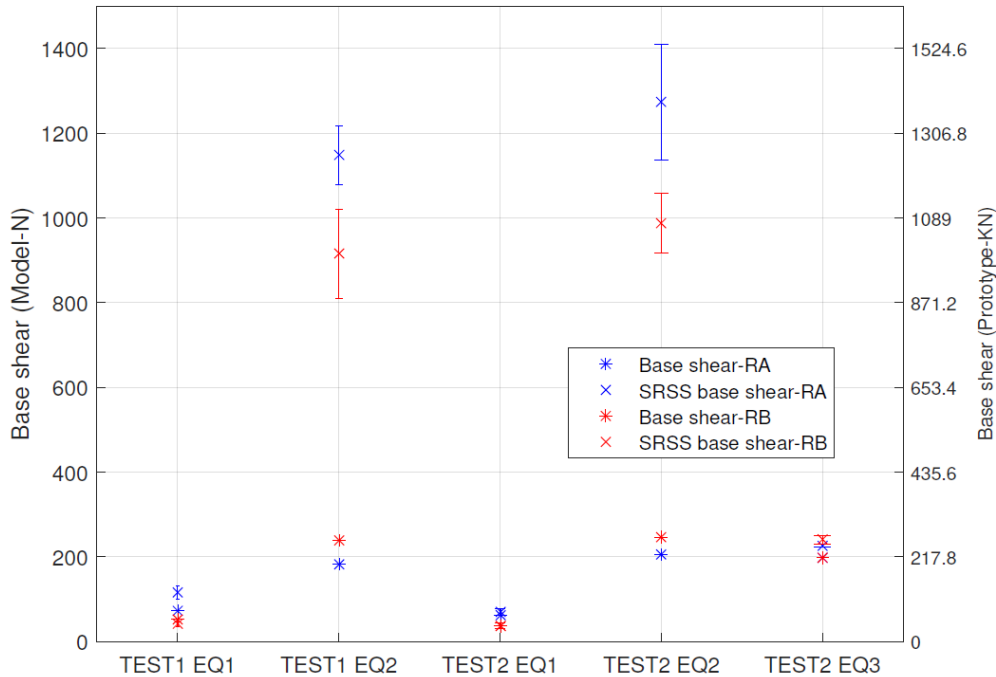


Figure 12: Base shear maxima from fixed base SRSS solution and as obtained from the centrifuge testing

BASE SHEAR DIFFERENCE (%)	TEST-1 EQ-1	TEST-1 EQ-2	TEST-2 EQ-1	TEST-2 EQ-2	TEST-2 EQ-3
RA	-38	-84	-13	-83	-13
RB	+23	-74	-2	-75	-18

Table 3: Percentage difference of the experimental base shear with respect to the average SRSS solution

- The manifestation of rocking was detected by observing large amplitude spike accelerations close to the pivot points, driven by the excitation frequency content.
- Internal loadings of the twin models reflected the global response in terms of storey shear and overturning moment and were bound between the same extrema, regardless of the extent of rotation during rocking. This indicates that, for the two models considered, structural rocking and foundation rocking produced very similar beneficial effect of reducing the superstructure force demand.
- The base isolation effect was evident during large amplitude excitations with a target excitation frequency matching the natural frequency of the models and during these, rocking with minor sliding was observed for both models. During a low frequency excitation, the response varied significantly between the two models due to different levels of sliding. However, more tests which cause larger amplitude rocking are needed to investigate further the role of rocking and the relative effects of any additional structural or soil energy dissipation.

REFERENCES

- [1] Marquis, F., Kim, J.J., Elwood, K.J., Chang, S.E., Understanding post-earthquake

- decisions on multi-storey concrete buildings in Christchurch, New Zealand. *Bulletin of Earthquake Engineering*, **15**, 731–758, 2017.
- [2] Franco, G., Siembieda, W., Chile's 2010 M8.8 earthquake and tsunami: Initial observations on resilience. *Journal of Disaster Research*, **5**, 577–590, 2010.
- [3] Housner, G.W., The behaviour of inverted pendulum structures during earthquakes. *Bulletin of Seismological Society of America*, **53**, 403–417, 1963.
- [4] Plaut, R.H., Fielder, W.T., Virgin, L.N., Fractal behavior of an asymmetric rigid block overturning due to harmonic motion of a tilted foundation. *Chaos, Solitons & Fractals*, **7**, 177–196, 1996.
- [5] Makris, N., A half-century of rocking isolation. *Earthquakes and Structures*, **7**, 1187–1221, 2014.
- [6] Ajrab, J.J., Pekcan, G., Mander, J.B., Rocking wall-frame structures with supplemental tendon systems. *Journal of Structural Engineering*, **130**, 895–903, 2004.
- [7] Ma, X., Deierlein, G., Eatherton, M., Krawinkler, H., et al., Large-scale shaking table tests of steel braced frame with controlled rocking and energy dissipating fuses. *Proceedings of the 9th U.S. National and 10th Canadian Conference on Earthquake Engineering*, 2010.
- [8] Hajjar, J.F., Sesen, H.A., Jampole, E., Wetherbee, A., *A synopsis of sustainable structural systems with rocking, self centering, and articulated energy-dissipating fuses*, Boston 2013.
- [9] Kelly, J.M., Skinner, R.I., Heine, A.J., Mechanisms of energy absorption in special devices for use in earthquake resistant structures. *Bulletin of the New Zealand Society for Earthquake Engineering*, **5**, 63–73, 1972.
- [10] Sharpe, R.D., Skinner, R.I., The seismic design of an industrial chimney with rocking base. *Bulletin of the New Zealand National Society for Earthquake Engineering*, **16**, 98–106, 1983.
- [11] Tyler, R.G., Tapered steel energy dissipators for earthquake resistant structures. *Bulletin of the New Zealand National Society for Earthquake Engineering*, **11**, 1978.
- [12] Acikgoz, S., Argyle, A., DeJong, M.J., The role of supplemental damping in limiting forces and displacements in a rocking structure. *Proceedings of the 2nd European Conference on Earthquake Engineering and Seismology*, 1–12, 2014.
- [13] Pollino, M., Bruneau, M., Seismic retrofit of bridge steel truss piers using a controlled rocking approach. *Journal of Bridge Engineering*, **12**, 600–610, 2007.
- [14] Tremblay, R., Poirier, L., Bouaanani, N., Leclerc, M., et al., Innovative Viscously Damped Rocking Braced Steel Frames. *The 14th World Conference on Earthquake Engineering (14 WCEE), October 12-17, 2008*.
- [15] Gajan, S., Saravanathiiban, D.S., Modeling of energy dissipation in structural devices and foundation soil during seismic loading. *Soil Dynamics and Earthquake Engineering*, **31**, 1106–1122, 2011.
- [16] Acikgoz, S., DeJong, M.J., The rocking response of large flexible structures to earthquakes. *Bulletin of Earthquake Engineering*, **12**, 875–908, 2013.
- [17] Acikgoz, S., Ma, Q., Palermo, A., DeJong, M.J., Experimental Identification of the

- Dynamic Characteristics of a Flexible Rocking Structure. *Journal of Earthquake Engineering*, **20**, 1199–1221, 2016.
- [18] Acikgoz, S., DeJong, M.J., Analytical modelling of multi-mass flexible rocking structures. *Earthquake Engineering & Structural Dynamics*, **45**, 2103–2122, 2016.
- [19] Vassiliou, M.F., Mackie, K.R., Stojadinović, B., Dynamic response analysis of solitary flexible rocking bodies: modeling and behavior under pulse-like ground excitation. *Earthquake Engineering & Structural Dynamics*, **43**, 1463–1481, 2014.
- [20] Wiebe, L., Christopoulos, C., Tremblay, R., Leclerc, M., Mechanisms to limit higher mode effects in a controlled rocking steel frame. 1: Concept, modelling, and low-amplitude shake table testing. *Earthquake Engineering & Structural Dynamics*, **42**, 1053–1068, 2013.
- [21] Wiebe, L., Christopoulos, C., A cantilever beam analogy for quantifying higher mode effects in multistorey buildings. *Earthquake Engineering & Structural Dynamics*, **44**, 1697–1716, 2015.
- [22] Gazetas, G., Apostolou, M., Nonlinear soil – structure interaction: Foundation uplifting and soil yielding. *Proceedings Third UJNR Workshop on Soil-Structure Interaction*, 1–16, 2004.
- [23] Loli, M., Knappett, J.A., Brown, M.J., Anastasopoulos, I., Gazetas, G., Centrifuge modeling of rocking-isolated inelastic RC bridge piers. *Earthquake Engineering & Structural Dynamics*, **43**, 2341–2359, 2014.
- [24] Deng, L., Kutter, B.L., Kunnath, S.K., Centrifuge modeling of bridge systems designed for rocking foundations. *Journal of Geotechnical and Geoenvironmental Engineering*, **138**, 335–344, 2012.
- [25] Gelagoti, F., Kourkoulis, R., Anastasopoulos, I., Gazetas, G., Rocking-isolated frame structures: Margins of safety against toppling collapse and simplified design approach. *Soil Dynamics and Earthquake Engineering*, **32**, 87–102, 2012.
- [26] Liu, W., Hutchinson, T.C., Gavras, A.G., Kutter, B.L., Hakhamaneshi, M., Seismic Behaviour of Frame-Wall-Rocking Foundation Systems. I: Test Program and Slow Cyclic Results. *Journal of Structural Engineering*, **141**, 4015059, 2015.
- [27] Gajan, S., Kutter, B.L., Capacity, settlement, and energy dissipation of shallow footings subjected to rocking. *Journal of Geotechnical and Geoenvironmental Engineering*, **134**, 1129–1141, 2008.
- [28] Heron, C.M., The Dynamic Soil Structure Interaction of Shallow Foundations on Dry Sand Beds. 2013.
- [29] CEN, Eurocode 7: Geotechnical design - Part 1: General rules 2004.
- [30] Acikgoz, S., DeJong, M.J., The interaction of elasticity and rocking in flexible structures allowed to uplift. *Earthquake Engineering & Structural Dynamics*, **41**, 2177–2194, 2012.